GEOPHYSICAL RESEARCH LETTERS, VOL. 35, L08104, doi:10.1029/2007GL032868, 2008

Modulated reconnection rate and energy conversion at the magnetopause under steady IMF conditions

L. Rosenqvist,[1] A. Vaivads,[1] A. Retinò,[1,2] T. Phan,[3] H. J. Opgenoorth,[4] I. Dandouras,[5] and S. Buchert[1]

Received 10 December 2007; revised 26 February 2008; accepted 6 March 2008; published 30 April 2008.

[1] We use the multi-spacecraft mission Cluster to make observational estimates of the local energy conversion across the dayside high-latitude magnetopause. The energy conversion is estimated during eleven complete magnetopause crossings under steady south-dawnward interplanetary magnetic field (IMF). We describe a new method to determine the reconnection rate from the magnitude of the local energy conversion. The reconnection rate as well as the energy conversion varies during the course of the eleven crossings and is typically much higher for the outbound crossings. This supports the previous interpretation that reconnection is continuous but its rate is modulated.
Citation: Rosenqvist, L., A. Vaivads, A. Retinò, T. Phan, H. J. Opgenoorth, I. Dandouras, and S. Buchert (2008), Modulated reconnection rate and energy conversion at the magnetopause under steady IMF conditions, *Geophys. Res. Lett.*, *35*, L08104, doi:10.1029/2007GL032868.

1. Introduction

[2] The efficiency of solar wind (SW)- magnetosphere (MSPH) coupling is thought to be controlled by the magnetic reconnection process at the magnetopause (MP) [*Dungey*, 1961]. One of the most important aspects of reconnection is the conversion between magnetic and particle energy. The conservation of electromagnetic energy is given by Poynting's theorem which can be written as,

$$\frac{\partial}{\partial t}\frac{B^2}{2\mu_0} + \nabla\cdot\vec{S} = -\vec{E}\cdot\vec{j} = -\vec{E}'\cdot\vec{j} - \left(\vec{j}\times\vec{B}\right)\cdot\vec{v}, \qquad (1)$$

using the electric field in the plasma rest frame (governed by the generalized Ohm's law), $\vec{E}' = \vec{E} + \vec{v}\times\vec{B}$ and neglecting the electric field energy density. Here $\vec{S} = \frac{\vec{E}\times\vec{B}}{\mu_0}$ is the Poynting vector and $\vec{E}\cdot\vec{j}$ gives the local energy conversion rate. The first term on the right corresponds to energy conversion due to non-ideal magnetohydrodynamic (MHD) effects while the second term governs the ideal MHD conversion between magnetic and kinetic (thermal and bulk flow) energy. In the ideal MHD limit a positive value of $(\vec{j}\times\vec{B})\cdot\vec{v}$ corresponds to a load, conversion from magnetic to kinetic energy, and vice versa to a generator if it is negative. Figure 1 illustrates the predicted load and generator regions around the MP for southward IMF.

[3] Usually, the energy input to the MSPH is evaluated using empirical coupling functions [e.g., *Akasofu*, 1979] in the upstream SW. However, recently *Rosenqvist et al.* [2006] estimated the global energy transfer across the MP based on direct measurements of the local energy conversion based on the physical relations above. This truly physical approach is optimized via the utilization of the Cluster multispacecraft mission. The local energy conversion Q is represented by

$$Q\left(\mathrm{Wm}^{-2}\right) = \int \left(\vec{j}\times\vec{B}\right)\cdot\vec{v}v_{mp}\mathrm{d}t. \qquad (2)$$

where v_{mp} is the velocity of the magnetopause. The local energy conversion can be separated into three components $\vec{F}\cdot\vec{v} = \vec{F}_n\cdot\vec{v}_{mp} + \vec{F}_n\cdot\vec{v}_n + \vec{F}_t\cdot\vec{v}_t$ ($\vec{F} = \vec{j}\times\vec{B}$). The first term represents the energy involved in the motion of the MP while the second and third term involves the energy conversion due to the plasma flow and/or forces normal and tangential to the MP respectively. Current in-situ measurements are, due to their limited spatial extent, inadequate to evaluate the loss or gain of the first term. We thus neglect this term, assuming that the oscillatory motion of the MP is approximately an adiabatic process.

[4] In this paper we study the local energy conversion across the MP, Q, during multiple MP crossings on 26 January 2001. The Cluster spacecraft (SC) were located in the high-latitude northern duskside MP with an inter-SC separation of about 650 km with SC1-3 orientated tangential to a model MP and SC4 closer to Earth (see Figure 1). The IMF was remarkably steady for over two hours (south-dawnward). This event has previously been studied by *Bosqued et al.* [2001] and *Phan et al.* [2004] which both found convincing signatures of continuously active reconnection. Eleven complete MP crossings between 10:29 UT and 11:05 UT where identified by *Phan et al.* [2004] during which high-speed plasma jets were detected by Cluster. This provides an excellent opportunity to study the energy conversion across the MP during an extended time interval when no influence from varying interplanetary conditions is expected. Our main goal is to study if, how and possibly why the energy conversion and reconnection rate varies in the course of the eleven crossings, as it should be important

[1]Swedish Institute of Space Physics, Uppsala, Sweden.
[2]Now at Space Research Institute, Austrian Academy of Sciences, Graz, Austria.
[3]Space Sciences Laboratory, University of California, Berkeley, California, USA.
[4]Solar System Mission Division, ESA/ESTEC, Noordwijk, Netherlands.
[5]CESR, Toulouse, France.

0094-8276/08/2007GL032868$05.00

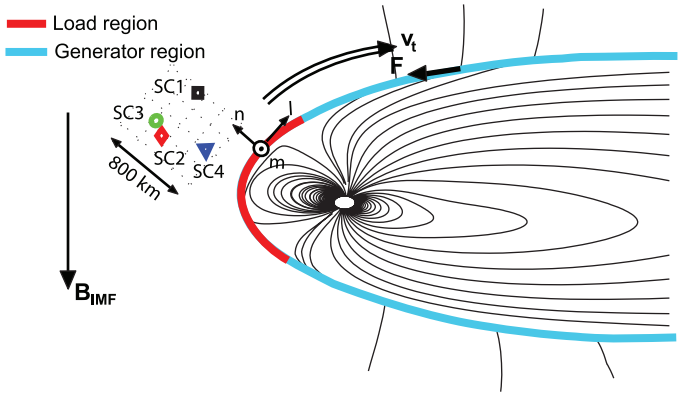

Figure 1. A schematic sketch of the load/generator regions around the MP during southward IMF. The Cluster configuration at 10:30 UT is shown in the *nml* reference frame.

for our understanding of the solar wind driving of the SW-MSPH coupling.

2. Overview of Observations

[5] To justify the neglect of all non-ideal MHD contributions in Equation 1 we have compared observations from different instruments on Cluster [see *Escoubet et al.*, 2001, and references therein]. We use data from the FGM, CIS, and EFW instruments. Plasma velocity data are obtained from CIS/CODIF on SC4 and CIS/HIA on SC1 with good agreement.

[6] An overview of the studied time interval is shown in Figure 2. The eleven complete MP crossings are coloured, blue marks the outbound MP crossings from MSPH to magnetosheath (MSH), and yellow marks the inbound crossings. The MP current layer is identified by a large change in B_z (Figure 2a). High-speed plasma jets are observed at all crossings except 10 (10 lacks ion measurements within the MP) and have been identified by *Phan et al.* [2004] as alfvénic reconnection jets.

[7] Figure 2c shows integrated values of the instantaneous power conversion $(\vec{j} \times \vec{B}) \cdot \vec{v}$ (blue line) and $\vec{E} \cdot \vec{j}$ (green line) where $\vec{j}$ and $\vec{B}$ are obtained from FGM, $\vec{v}$ from CIS and $\vec{E}$ from EFW with 4 s resolution and assuming $\vec{E} \cdot \vec{B} = 0$. A closer examination of the magnetic field data from all four SC reveals that sometimes the current sheet is thinner (<650 km) than the inter-SC separation, thus the curlometer method is not applicable for estimating $\vec{j}$ for such crossings. Instead single-SC current estimations have been used based on a model boundary normal, n = [0.7, 0.43, 0.50] [*Shue et al.*, 1998] and an average v_{mp} = 40 km/s [*Bosqued et al.*, 2001]. The assumption of v_{mp} is not of critical importance as it affects the magnitude of both curves equally and we are interested in their difference. The iongyroradius is ~50 km and thus we measure on a scale of a few iongyroradii which is smaller than the typical thickness of the current sheet, ~1000 km [*Bosqued et al.*, 2001]. Figure 2c shows the good agreement between the two different methods. Only at the end of the interval the differences approach 50%. Thus, it seems like the $(\vec{j} \times \vec{B}) \cdot \vec{v}$ term is dominating the overall energy conversion. This is also supported by kinetic simulations of reconnection in the magnetotail [*Birn and Hesse*, 2005].

3. Results

3.1. Local Energy Conversion

[8] The energy conversion is dominantly positive over the entire time period (Figure 2c), thus corresponding to a load in the GSE reference frame. To investigate the variation during the course of the eleven crossings we must evaluate the energy conversion at each crossing separately. As v_n is small, associated with large uncertainties, and difficult to separate from v_{mp} we neglect the contribution from $\vec{F}_n \cdot \vec{v}_n$ to Equation 2 in this paper. This is justified because for rotational discontinuities expected for MP crossings during ongoing reconnection $F_n \approx 0$. However, in the few crossings where it is possible to estimate, $F_n \approx F_t$ (not shown). Although $\vec{F}_n \cdot \vec{v}_n$ can still be neglected since $v_t \gg v_n$. Thus we need to determine the MP boundary normal for each crossing in order to estimate the velocity component tangential to the MP entering Equation 2.

[9] Figure 3 shows observations from the first outbound crossing. Figure 3a shows the B_x for all four SC. It is seen that the current sheet thickness varies during the crossing, sometimes all SC can be inside the current sheet (thick current sheet, e.g., ~10:31:50 UT) and sometimes the SC can be on opposite sides of the current sheet (thin current sheet, e.g., ~10:31:35 UT). This indicates that the MP is rippled by bulges, as already suggested by *Phan et al.* [2004]. Thus, neither the 4-SC timing technique nor the curlometer method is applicable. However, single-SC current estimates obtained using MP normals from minimum variance analysis (MVA) can be used since the dependence on the MP velocity cancels as we integrate over the MP width in Equation 2. On the other hand, also the MVA proved to be difficult under such structured MP conditions. Therefore, we decided to perform the MVA on nested data segments centred at or near the actual current sheet crossing to investigate the time-stationarity of the normal vector. The SC (SC1 or SC4) that is least influenced by bulges during the crossing and consequently with the most reliable boundary normal estimations (highest ratio of the medium to minimum eigenvalues, L2/L3) is selected to evaluate the energy conversion. The normal direction is determined as the average over the time period when the nested analysis give similar results.

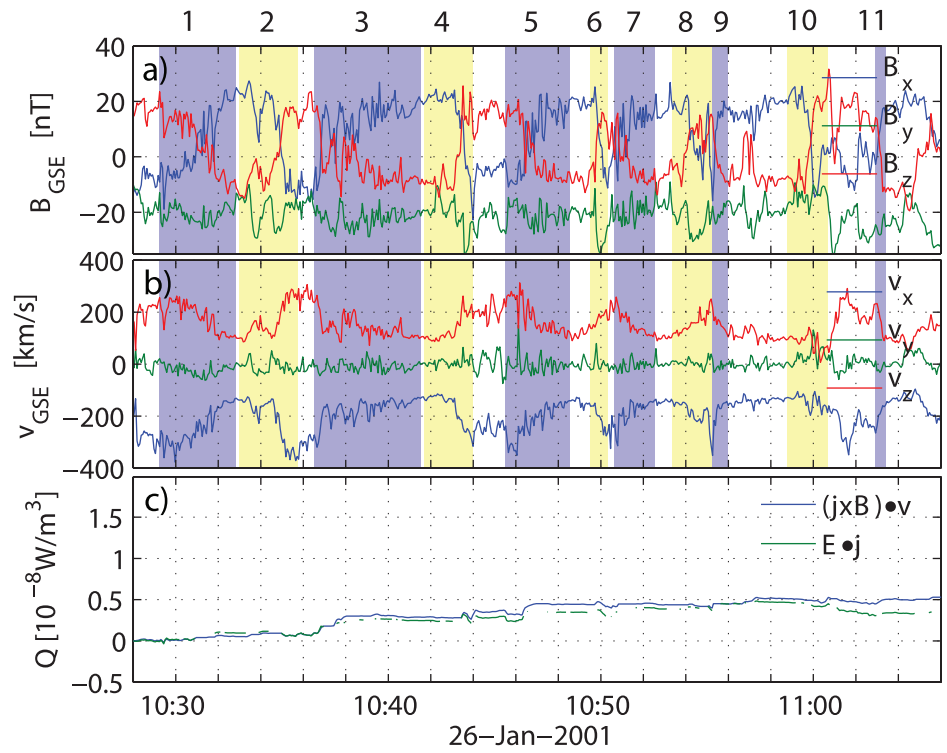

Figure 2. Overview of the event for SC1. The blue shaded areas correspond to outbound crossings, and yellow corresponds to inbound crossings.

Furthermore, we calculate the statistical uncertainty in the normal magnetic field component, B_n [*Sonnerup and Scheible*, 1998] and average the error over the nested segments. The relative error in Q is proportional to the relative error in B_n and considered to be the dominant uncertainty in the estimations. The first eight columns of Table 1 show for each of the eleven crossings, the SC used to evaluate Q_i (where subscript i indicates the number of the crossing), the start time of the MP crossing and duration, the MP normal (GSE), L2/L3, the average B_n and also its relative error.

[10] Figure 3b shows the magnetic field components for SC4 in the MP reference frame. It is evident that B_n is mostly less than zero consistent with reconnection taking place equatorward of Cluster. B_l changes from positive to negative, which indicates a crossing from the MSPH to the MSH. The current is mainly in the positive m-direction (Figure 3c). Note that we have assumed v_{mp} = 40 km/s to estimate j. The tangential velocity is mainly in the positive l-direction along the MP as shown in Figure 3d and consequently Q_1 is positive (Figure 3e) as expected. The energy conversion (Q_1) has been evaluated using both the model normal (green line) and the normal deduced from the nested variance technique (blue line) with good agreement. It is seen that the energy conversion mainly takes place at the centre of the current layer, thus the technique is not very sensitive to the definition of the start and end of the MP. Partial crossings (in/out) can also be seen in Q_1 (e.g., between 10:31:10 and 10:31:35). However, the resulting effect does not significantly influence the final Q_1 value.

[11] The result of the estimated MP energy conversion for each crossing is given in the 9th column of Table 1 and is summarized in Figure 4a together with the relative error. During crossing 4, 6 and 8 the MP is thick and it is possible to use the 4-SC timing method as well as the curlometer technique.

Table 1. Magnetopause Parameters for the Eleven Crossings

i = 1, .. , 11	s/c	Start Time, hh:mm:ss	Duration, m:ss	$\vec{n}$, GSE	$\langle$L2/L3$\rangle$	$\langle B_n \rangle$, nT	$\lvert\Delta B_n\rvert/\lvert B_n\rvert$	Q_i, mW/m^2	R_{Bn}	R_Q
1	B4	10:29:55	2:53	[0.51, 0.58, 0.64]	1.5	−5	1.4	0.067	0.2	0.3
2	B4	10:33:00	2:45	[0.59, 0.28, 0.76]	6.1	0.7	2.2	−0.007	0.04	-
3	B4	10:36:30	5:00	[0.62, 0.52, 0.59]	1.6	−5.6	0.94	0.05	0.2	0.19
4	B4	10:41:40	2:18	[0.75, 0.28, −0.60][a]	-	−0.3	-	0.009	0.01	0.03
5	B1[b]	10:45:32	3:01	[0.69, 0.38, 0.62]	21.5	−1.7	0.57	0.038	0.06	0.17
6	B4[b]	10:49:30	0:50	[0.52, 0.47, 0.71]	5.1	−3	0.71	0.02	0.1	0.05
7	B4	10:50:36	1:56	[0.58, 0.63, 0.51]	2.6	−6.4	0.63	0.065	0.26	0.4
8	B4	10:53:20	1:10	[−0.01, 0.45, 0.89][a]	-	−5.8	-	0.01	0.2	0.03
9	B1	10:55:15	0:45	[0.43, 0.52, 0.75]	5.5	−7.5	0.3	0.06	0.3	0.3
10	B4	10:58:44	2:17	[0.58, 0.36, 0.73]	9	0.62	1.97	0.00057	0.03	0.002
11	B4	11:03:10	0:30	[0.70, 0.40, 0.59]	50	−3.9	0.38	0.023	0.14	0.08

[a]The normal is estimated from timing.
[b]The data have been smoothed for the MVA.

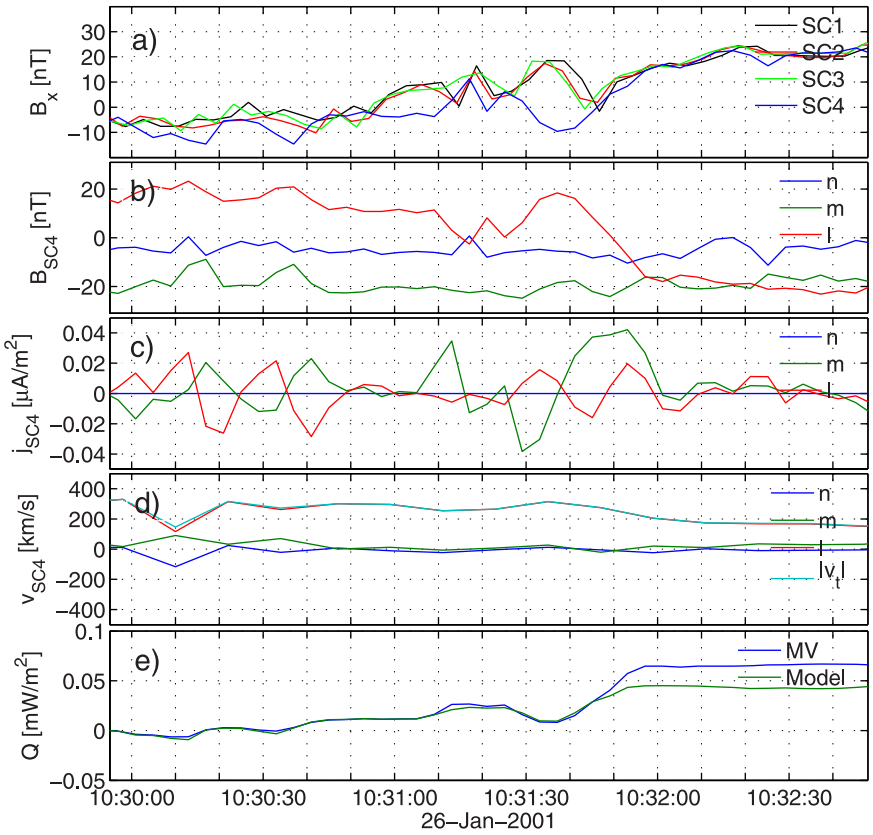

Figure 3. Summary of event 1. (a) B_x in GSE, (b) the magnetic field, (c) the current density, (d) the velocity for SC4, and (e) the integrated power conversion.

[12] It appears that the MVA is problematic for the first four crossings considering the very low L2/L3 value and rather large error bars. This sometimes results in an apparent flip of the m and n direction which is the case for crossing 4 and 8. Thus, we have used timing estimates for these crossings which seem to be more reliable than MVA. For the majority of the later crossings the MVA appears to provide more reliable results. Thus, we conclude that no technique works best for all crossings but instead the most reliable technique must be chosen on a case by case basis.

[13] By closer examination of these last crossings one finds that even when taking the error bars into account the energy conversion varies during the course of the crossings. This can be considered rather surprising as the interplanetary conditions are stable. Thus, some other mechanism must be responsible for the movement of the MP and the energy conversion variation.

3.2. Reconnection Rate

[14] The reconnection rate can be estimated from the observed Q_i estimates obtained above. Considering the ideal MHD, steady state Poynting theorem in integral form:

$$-\int_S \left(\frac{\vec{E}\times\vec{B}}{\mu_0}\right) d\vec{S} = \int_V (\vec{j}\times\vec{B})\cdot\vec{v}\, dV, \tag{3}$$

[15] Equation 3 can be written as,

$$\frac{B_0^2 v_{in}}{\mu_0} = \frac{1}{2}\langle(\vec{j}\times\vec{B})\cdot\vec{v}\rangle\Delta x, \tag{4}$$

assuming the same magnetic field magnitude on both sides of the current sheet, which is a good assumption in our case, and using $\vec{E} = -\vec{v}\times\vec{B} \Rightarrow E = -v_{in}B_0$. Here, v_{in} is the inflowing plasma velocity and B_0 the background magnetic field. Furthermore $\Delta V = \Delta S\,\Delta x$, ΔS being the surface area element and Δx being the width of the magnetopause. Comparing the right-hand side of Equation 4 with Equation 2 we realize that it is equal to $\frac{Q_i}{2}$ since $\Delta x = v_{mp}\Delta t$. Now using the definition of the reconnection rate,

$$R = \frac{v_{in}}{v_{A,in}} \tag{5}$$

where $v_{A,in}$ is the Alfvèn velocity in the inflow region defined as, $v_{A,in} = \frac{B_0}{\sqrt{\rho\mu_0}}$, and $v_{in} = \frac{Q_i\mu_0}{2B_0^2}$ from Equation 4 we can express the reconnection rate as,

$$R_Q = \frac{1}{2}\frac{Q_i}{\rho v_{A,in}^3}. \tag{6}$$

[16] Thus, we can calculate the reconnection rate based on the local energy conversion estimates for each crossing obtained in Section 4.1. The plasma density is obtained

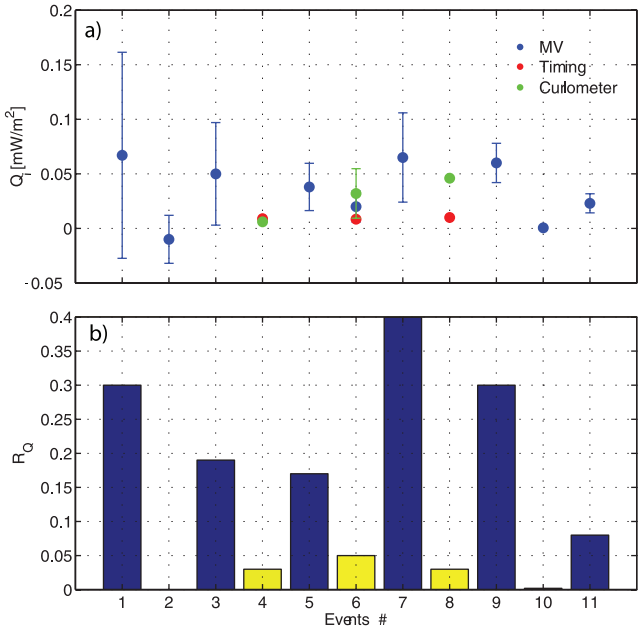

Figure 4. (a) The power conversion for each of the eleven crossings based on single s/c current estimation using MVA (blue) and timing (red) normals. The estimate based on the curlometer technique (green) is shown for the crossings where it is applicable. (b) The reconnection rate for all eleven crossings (blue bars indicate outbound and yellow bars indicate inbound crossings).

from the SC potential [*Pedersen et al.*, 2001]. The results are shown in the second to last column in Table 1 and in Figure 4b. For comparison, the reconnection rate based on B_n observations, $R_{Bn} = \frac{|B_n|}{B}$, is also shown in the last column in Table 1. R_Q is found to vary with a mean for all crossings of 0.17. Considering the uncertainties in obtaining such values, they are in rather good agreement with previous values of $\sim$0.1 [e.g., *Lindqvist and Mozer*, 1990]. Furthermore, one can note that the reconnection rate is always higher for the outbound crossings. Active reconnection occurring equatorwards of the SC peals off magnetic flux from the dayside which should result in a contraction of the MSPH. The lower reconnection rate for the inbound crossings may consequently indicate a decrease in the reconnection rate resulting in a relaxation of the MSPH. However, other explanations are possible, for example, a compression of the MSH against the MP may cause a thinner MP current which could enhance the reconnection rate (and vice versa). However, it is beyond the scope of the paper to investigate this matter further.

[17] The advantage of using R_Q lies in the possibility to directly obtain the tangential component of the Lorentz force by 4-sc techniques. If the tangential part is relatively large compared to the magnitude of the force it is not very sensitive to small variations in the normal direction. However, quantities that are small compared to the magnitude of the vector such as v_{in} and B_n are sensitive to small variations in the normal direction. Therefore, the use of 4-sc techniques can significantly reduce the relative error of R_Q in comparison to R_{Bn}. However, for the majority of the MP crossings we were forced to use single-SC current density estimates making R_Q directly proportional to B_n. Thus, in this case the relative errors of R_Q and R_{Bn} are the same. The estimations of R_{Bn} and R_Q agree well in most crossings according to Table 1 except for crossing 8 and 10 where they differ by an order of magnitude. This is because the method to obtain R_Q considers the real speed of the outflowing high-speed plasma instead of assuming the jets to be alfvénic as in R_{Bn}. At least, crossing 10 is characterised by the absence of high-speed flows. Thus, when there is a substantial deviation from alfvénic plasma flow the method based on the energy conversion estimates is more reliable despite the limitation of using single-SC current measurements. Note, however, that in the diffusion region MHD is not valid and thus both methods are inadequate there.

4. Conclusions

[18] The analysis of the multiple MP crossings on the 26 of January 2001 suggests the following:

[19] 1. The energy conversion has been estimated for eleven complete MP crossings characterised by high-speed reconnection jets. In most cases Cluster observes a load region, conversion from magnetic to particle energy, as the reconnected field lines contract and accelerate the plasma.

[20] 2. During this event the MP surface is rippled with the presence of bulges. We use different methods to estimate boundary properties and current densities. No method works best for all crossings but the most appropriate one should be chosen, depending on the nature of the crossing.

[21] 3. The results indicate that the energy conversion rate change during the course of the eleven crossings. This supports the previous interpretation that reconnection is continuous, but its rate is modulated even when interplanetary conditions are steady.

[22] 4. A new method to estimate the dimensionless reconnection rate based on the observed local energy conversion rate across the MP has been developed. The advantage of this method is that it does not rely on determining rather small quantities. It also takes into account that reconnection jets are not always alfvénic.

[23] 5. The reconnection rate varies and is typically larger for the outbound crossings. One interpretation that is consistent with the observed magnetopause motion is that active reconnection peals off magnetic flux from the dayside resulting in a contraction of the MSPH. The subsequent MP relaxation could be a consequence of a decreased reconnection activity.

[24] **Acknowledgments.** LR and AR are supported by the Swedish National Space Board, and AV is supported by the Swedish Research Council.

References

Akasofu, S.-I. (1979), Energy coupling between the solar wind and the magnetosphere, *Planet Space Sci.*, *27*, 425–431.

Birn, J., and M. Hesse (2005), Energy release and conversion by reconnection in the magnetotail, *Ann. Geophys.*, *23*, 3365–3373.

Bosqued, J. M., et al. (2001), Cluster observations of the high-latitude magnetopause and cusp: Initial results from the CIS ion instrument, *Ann. Geophys.*, *19*, 1545–1566.

Dungey, J. W. (1961), Interplanetary magnetic field and the auroral zones, *Phys. Rev. Lett.*, *6*, 47–48, doi:10.1103/PhysRevLett.6.47.

Escoubet, C. P., M. Fehringer, and M. Goldstein (2001), The Cluster mission, *Ann. Geophys.*, *19*, 1197–1200.

Lindqvist, P.-A., and F. S. Mozer (1990), The average tangential electric field at the noon magnetopause, *J. Geophys. Res.*, *95*, 17,137–17,144.

Pedersen, A., et al. (2001), Four-point high time resolution information on electron densities by the electric field experiments (EFW) on Cluster, *Ann. Geophys.*, *19*, 1483–1489.

Phan, T. D., et al. (2004), Cluster observations of continuous reconnection at the magnetopause under steady interplanetary magnetic field conditions, *Ann. Geophys.*, *22*, 2355–2367.

Rosenqvist, L., S. Buchert, H. J. Opgenoorth, A. Vaivads, and G. Lu (2006), Magnetospheric energy budget during huge geomagnetic activity using Cluster and ground-based data, *J. Geophys. Res.*, *111*, A10211, doi:10.1029/2006JA011608.

Shue, J. H., et al. (1998), Magnetopause location under extreme solar wind conditions, *J. Geophys. Res.*, *103*, 17,691–17,700.

Sonnerup, B. U., and M. Scheible (1998), Minimum and maximum variance analysis, in *Analysis Method for Multi-Spacecraft Data*, edited by G. Paschmann and P. W. Daly, pp. 185–220, Eur. Space Agency, Paris.

S. Buchert, L. Rosenqvist, and A. Vaivads, Swedish Institute of Space Physics, Lagerhyddsvagen 1, SE-751 21 Uppsala, Sweden. (lisa.rosenqvist@irfu.se)

A. Retinò, Space Research Institute, Austrian Academy of Sciences, A-8042 Graz, Austria.

I. Dandouras, CESR, BP 44346, F-31028 Toulouse, France.

H. J. Opgenoorth, Solar System Mission Division, ESA/ESTEC, P.O. Box 299, NL-2200 AG Noordwijk, Netherlands.

T. Phan, Space Sciences Laboratory, University of California, Berkeley, Berkeley, CA 94720, USA.